Since January 2020 Elsevier has created a COVID-19 resource centre with free information in English and Mandarin on the novel coronavirus COVID-19. The COVID-19 resource centre is hosted on Elsevier Connect, the company's public news and information website.

Virology 505 (2017) 42–55

Contents lists available at ScienceDirect

Virology

journal homepage: www.elsevier.com/locate/yviro

Nuclear imprisonment of host cellular mRNA by nsp1β protein of porcine reproductive and respiratory syndrome virus

Mingyuan Han[1], Hanzhong Ke, Qingzhan Zhang, Dongwan Yoo*

Department of Pathobiology, University of Illinois at Urbana-Champaign, 2001 South Lincoln Avenue, Urbana, IL 61802, USA

ARTICLE INFO

Keywords:
PRRSV
Interferon suppression
MRNA nuclear export
Nsp1
Arterivirus
SAP motif
Pathogenesis

ABSTRACT

Positive-strand RNA genomes function as mRNA for viral protein synthesis which is fully reliant on host cell translation machinery. Competing with cellular protein translation apparatus needs to ensure the production of viral proteins, but this also stifles host innate defense. In the present study, we showed that porcine reproductive and respiratory syndrome virus (PRRSV), whose replication takes place in the cytoplasm, imprisoned host cell mRNA in the nucleus, which suggests a novel mechanism to enhance translation of PRRSV genome. PRRSV nonstructural protein (nsp) 1β was identified as the nuclear protein playing the role for host mRNA nuclear retention and subversion of host protein synthesis. A SAP (SAF-A/B, Acinus, and PIAS) motif was identified in nsp1β with the consensus sequence of $_{126}$-LQxxLxxxGL-$_{135}$. In situ hybridization unveiled that SAP mutants were unable to cause nuclear retention of host cell mRNAs and did not suppress host protein synthesis. In addition, these SAP mutants reverted PRRSV-nsp1β-mediated suppression of interferon (IFN) production, IFN signaling, and TNF-α production pathway. Using reverse genetics, a series of SAP mutant PRRS viruses, vK124A, vL126A, vG134A, and vL135A were generated. No mRNA nuclear retention was observed during vL126A and vL135A infections. Importantly, vL126A and vL135A did not suppress IFN production. For other arteriviruses, mRNA nuclear accumulation was also observed for LDV-nsp1β and SHFV-nsp1β. EAV-nsp1 was exceptional and did not block the host mRNA nuclear export.

1. Introduction

Porcine reproductive and respiratory syndrome (PRRS) emerged in the United States in 1987 and subsequently in Europe in 1990, and has since become endemic in most pig-producing countries worldwide (Benfield et al., 1992; Wensvoort et al., 1991). The etiological agent is PRRS virus (PRRSV) that falls into the family *Arteriviridae* together with lactate dehydrogenase-elevating virus (LDV) of mice, equine arteritis virus (EAV), and simian hemorrhagic fever virus (SHFV). The PRRSV genome is a single-stranded positive-sense RNA of 15 Kb in length with the 5′ cap and the 3′-polyadenylated [poly(A)] tail (Meulenberg et al., 1993; Nelsen et al., 1999; Wootton et al., 2000). Two large open reading frames (ORFs), ORF1a and ORF1b, occupy the 5′ three-quarters of the genome and code for two polyproteins, pp1a and pp1ab, with the expression of the latter mediated by −1 frame-shifting in the ORF1a/ORF1b overlapping region (Snijder and Meulenberg, 1998). The pp1a and pp1ab proteins are further processed to generate 14 nsps. The remaining sequence is located in the 3′ one-quarter of the genome codes for structural proteins (Firth et al., 2011; Johnson et al., 2011; Nelsen et al., 1999; Wootton et al., 2000). A −2 ribosomal frame-shifting has recently been identified for expression of nsp2TF in the nsp2-coding region (Fang et al., 2012).

Host innate immune system produces cytokines and chemokines in response to PRRS viral infection for protection (Yoo et al., 2010). However, poor induction of proinflammatory cytokines and type I IFNs has been shown as the hallmark of PRRSV infection in cells and pigs (For a review, see Han and Yoo (2014), Sun et al. (2012)). A decrease of IFN transcripts is observed in PRRSV-infected MARC-145 cells (Miller et al., 2004). On the contrary, IFN-α mRNA is augmented after stimulation in PRRSV-infected macrophages, suggesting that a post-transcriptional event may be involved in regulating the IFN response".

(Lee et al., 2004; Miller et al., 2009). NF-κB suppression is likely involved in down-regulation of IFN production during early infection of PRRSV. At downstream, CREB (cyclic AMP responsive element binding)-binding protein (CBP) is degraded by PRRSV and thus the assembly of enhanceosome for IFN transcription is disrupted (Kim et al., 2010).

In addition to modulating host cell signaling, the seizing of host

* Corresponding author.
E-mail addresses: hanming@umich.edu (M. Han), dyoo@illinois.edu (D. Yoo).
[1] Present address: Department of Pediatrics & Communicable Diseases University of Michigan, Ann Arbor, MI 48109-5688, USA.

http://dx.doi.org/10.1016/j.virol.2017.02.004
Received 16 November 2016; Received in revised form 3 February 2017; Accepted 8 February 2017
Available online 20 February 2017
0042-6822/

protein synthesis is a complementary strategy for a virus to suppress host innate defense (Walsh and Mohr, 2011). Viral replication relies on the translation machinery of cells, and commandeering ribosomes to viral mRNA is essential for viral protein expression, genome replication, and progeny virus production. Discrete viral strategies for subversion of cellular mRNA translation have been uncovered, which include interference on translation factors (Walsh and Mohr, 2011), cellular mRNA nuclear imprisonment (Kuss et al., 2013), cleavage of cellular mRNAs (Kamitani et al., 2006; Sokoloski et al., 2009), and induction of microRNAs (Abraham and Sarnow, 2011). For instance, inhibition of cap-dependent host protein translation has been well studied for member viruses of the order *Picornavirales*. Besides, some of picornaviruses impede host protein translation by blocking the nucleocytoplasmic trafficking of cellular mRNA (Kuss et al., 2013).

For viruses in the *Nidovirales* order, the SARS-CoV nsp1 inhibits the expression of host genes (Huang et al., 2011b). SARS-CoV nsp1 induces the cleavage of host mRNAs and binds to 40S ribosomes to inactivate their translation functions (Kamitani et al., 2009, 2006). The nsp1 of mouse hepatitis virus (MHV) and transmissible gastroenteritis virus (TGEV) strongly reduces cellular mRNA expression but the strategy used by TGEV nsp1 differs from that of SARS-CoV nsp1 (Huang et al., 2011a; Tohya et al., 2009; Zust et al., 2007). For arteriviruses, modulation of host protein synthesis is poorly understood. In the present study, we demonstrated that PRRSV imprisoned host cellular mRNA in the nucleus, which was mediated by nsp1β, implying an enhanced access to host translation apparatus for viral mRNAs in the cytoplasm. A conserved motif for SAP (SAF-A/B, Acinus, and PIAS) was identified in the nsp1β subunit and this motif played multiple roles for nuclear distribution of nsp1β, mRNA nuclear accumulation, subversion of host protein synthesis, innate immune responses, and PRRSV replication.

2. Materials and methods

2.1. Cells and viruses

HeLa cells (NIH AIDS Research and Reference Reagent Program, Germantown, MD), MARC-145 cells, and RAW 264.7 cells were grown in Dulbecco's modified Eagle's medium (DMEM; Mediatech Inc., Manassas, VA), supplemented with 10% heat-inactivated fetal bovine serum (FBS; HyClone, Logan, UT) in a humidified incubator with 5% CO2 at 37 °C. North American (NA) type PRRSV strains VR-2332, PA8, and NVSL 97–7895 (FL12), and European (EU) type PRRSV strain Lelystad virus (LV) were propagated in MARC-145 cells and used as virus stocks for the present study. For infection, MARC-145 cells were grown to approximately 70% confluency and infected at a multiplicity of infection (moi) of 0.1–5. Vesicular stomatitis Indiana virus expressing green fluorescent protein (VSIV-GFP) (Dalton and Rose, 2001) was kindly provided by Adolfo García-Sastre (Mt. Sinai School of Medicine, New York, NY).

2.2. Antibodies and chemicals

An anti-PRRSV-nsp1β rabbit pAb specific for NA-PRRSV nsp1β was generated at the Immunological Research Center, University of Illinois at Urbana-Champaign (Urbana, IL). The anti-LV-nsp2/3 antibody was a generous gift from E. Snijder, (Leiden University Medical Center, Leiden, Netherlands). Anti-N protein mAbs (SDOW17) was obtained from E. Nelson (South Dakota State University, Brookings, SD). polyinosinic: polycytidylic [poly (I:C)], DAPI (4′,6-diamidino-2-phenylindol), anti-Flag mAb (F3165), and anti-FLAG pAb (F7425) were purchased from Sigma (St. Louis, MO). Anti-β-actin mAb (sc-47778), anti- HSP90 mAb (sc-69703), and anti-PARP pAb (sc-7150) were purchased from Santa Cruz Biotechnologies Inc. (Santa Cruz, CA). Anti-ISG15 pAb and anti-GFP pAb were purchased from Thermo Scientific (Rockford, IL). Anti-DEPTOR pAb was purchased from Invitrogen (Carlsbad, CA). The peroxidase-conjugated Affinipure goat anti-mouse IgG and peroxidase-conjugated Affinipure goat anti-rabbit IgG were purchased from Jackson Immuno Research (West Grove, PA). Alexa-Flour 488-conjugated and Alexa-Flour 568-conjugated secondary antibodies were purchased from Invitrogen.

2.3. Plasmids and DNA transfection

Construction of plasmids expressing individual arterivirus nsp1 subunits were described previously (Han et al., 2013, 2014; Han and Yoo, 2014; Song et al., 2010). Mutant genes were generated by PCR-based site-directed mutagenesis using specific primers (Table S1). The reporter plasmids pIFN-β-Luc and p4xIRF3-Luc were kindly provided by Stephan Ludwig (Institute of Molecular Medicine, Heinrich Heine Universtät, Düsseldorf, Germany) (Ehrhardt et al., 2004) and used for luciferase assays. The plasmid pPRDII-Luc was provided by Stanley Perlman (University of Iowa, Ames, IA). The plasmid pISRE-Luc was purchased from Stratagene (La Jolla, CA). The plasmid pswTNF-α-luc was provided by Fernando Osorio (University of Nebraska-Lincoln, Lincoln, NE). The *Renilla* luciferase plasmid pRL-TK was included to serve as an internal control in luciferase reporter assay (Promega). The plasmid pEGFP-N1 (Clontech) was used for GFP co-expression. The plasmids pDsRed2-Mito and pDsRed2-ER were used as subcellular compartmental markers for mitochondria (MITO) and endoplasmic reticulum (ER), respectively (Clontech). DNA transfection was performed using Lipofectamine 2000 according to the manufacturer's instructions (Invitrogen).

2.4. Western blot analysis

Cells were lysed using the M-PER® mammalian protein extraction reagent (Thermo Scientific, Rockford, IL) supplemented with a cocktail of protease inhibitors (P-8340 Sigma). Cell lysates were centrifuged and supernatants were resolved by 10% or 12% sodium dodecyl sulfate (SDS)-poly-acrylamide gel electrophoresis and transferred to polyvinylidene fluoride (PVDF) membrane (Millipore). After blocking with 5% skim milk powder in TBS-T (10 mM Tris–HCl [pH 8.0], 150 mM NaCl, 1% Tween 20), membranes were incubated with primary antibody diluted in TBS-T containing 5% skim milk powder for 1 h at R/T followed by washing and incubation with horseradish peroxidase-conjugated secondary antibody for 1 h at R/T. After three washes with TBS-T, protein bands were visualized using the Enhanced Chemiluminescence immunoassay system (Thermo Scientific).

2.5. Immunofluorescence analysis (IFA)

Cells for IFA were fixed with 4% paraformaldehyde for 10 min at R/T in (PBS) and then permeabilized using 0.1% Triton X-100 for 10 min at R/T. After blocking with 1% BSA in PBS for 30 min, cells were incubated with primary antibody in PBS containing 1% BSA for 2 h followed by incubation with secondary antibody for 1 h. The nucleus was stained with DAPI (4′,6-diamidino-2-phenylindole) for 3 min at R/T. After washing with PBS, coverslips were mounted on microscope slides using the Fluoromount-G mounting medium (Southern Biotech, Birmingham, AL), and examined under LSM700 confocal laser scanning microscopy (Zeiss). Images were processed with NIH Image/J to determine fluorescence intensity (FI).

2.6. Generation of SAP mutant full-length PRRSV cDNA clones and mutant viruses

The infectious clone pFL12 was modified to generate pFL13 of which the T7 promoter was replaced with the CMV promoter. To modify the SAP motif of nsp1β ($_{124}$-KxLQxxLxxxGL-$_{135}$ for FL12 strain), PCR-based site-directed mutagenesis was conducted to substitute selected codons to alanine using the shuttle plasmid pFL13-SP-

nsp1 and primer pairs (Table S1). PCR-based mutagenesis was performed using QuikChange II XL Site-Directed Mutagenesis Kit (Agilent, Santa Clara, CA). The wild-type full-length genomic cDNA clone was digested with *AscI* and *SpeI*, and the fragment was replaced with the corresponding fragment obtained from the mutagenized shuttle plasmid.

MARC-145 cells were seeded in 35-mm-diameter dishes and grown to 70% confluency. Cells were transfected for 24 h with 2 μg of individual full-length clones using Lipofectamine 2000. Transfected cells were incubated for 5 days in DMEM supplemented with 10% FBS. The culture supernatants were harvested at 5 days post-transfection and designated 'passage-1′. The passage-1 virus was used to inoculate fresh MARC-145 cells, and the 5-day harvest was designated 'passage-2′. The 'passage-3′ virus was prepared in the same way as for passage-2. Each passage virus was aliquoted and stored at 80 °C until use. Viral titers were calculated using $TCID_{50}$ in MARC-145 cells.

2.7. Luciferase reporter assay

HeLa cells were transfected with various combinations of plasmid DNA: 0.5 μg of viral protein coding plasmid, 0.5 μg of reporter plasmid, and 0.05 μg of pLR-TK. At 24 h post-transfection, cells were stimulated with 0.5 μg of poly(I:C) by transfection for 16 h and cell lysates were prepared for luciferase assays. For pISRE-Luc, cells were incubated with 1,000 units of human IFN-β (bioWORLD, Dublin, OH) for 16 h. Raw264.7 cells were used for pswTNF-α-luc as described previously (Subramaniam et al., 2010). Luciferase activities were measured using the Dual-Glo Luciferase assay system according to the manufacturer's instruction (Promega). Values for each sample were normalized using *Renilla* luciferase activities and the results were expressed as relative luciferase activities. All assays were repeated at least three times, and each sample was analyzed in triplicate.

2.8. Real time quantitative PCR (RT-qPCR)

Total cellular RNA was extracted for RT-qPCR using RNeasy mini kit according to manufacturer's instruction (QIAGEN, Hilden, Germany). Nuclear and cytoplasmic RNAs were separated using SureprepTM cytoplasmic and nuclear RNA purification kit in accordance with the manufacturer's instruction (Fisher BioReagents, PA). RT-qPCR reactions were performed in the ABI sequence detector system (ABI Prism 7000 and software; Applied Biosystems). Primers for PRRSV N gene, *GADPH, DEPTOR, NOL6, SH2* were reported previously (Sun et al., 2014). The mRNA levels of indicated genes were calculated based on ΔΔCt method and normalized to that of *GAPDH* mRNA. Cytoplasmic and nuclear mRNA was normalized with total *GAPDH* mRNA (combination of cytoplasmic and nuclear fractions). Two independent experiments were conducted in triplicate each and the average of normalized values obtained from each infection and transfection experiment was determined.

2.9. Oligo(dT) in situ hybridization (ISH)

Oligo (dT) in situ hybridization was performed as described elsewhere (Chakraborty et al., 2006). Briefly, cells grown on cover slips were fixed for 8 min with 4% paraformaldehyde, permeabilized with 0.5% Triton X-100, and labeled with primary antibodies at chosen times after transfection or infection. The primary antibodies were diluted in PBS containing 0.2% Triton X-100, 1 mM DTT, and 200 U/ml RNasin (Promega). Cells were fixed again with paraformaldehyde and washed with PBS. Oligo (dT) in situ hybridization was then performed at 42 °C overnight with biotinylated oligo(dT) (Promega, WI). The cells were washed twice with 0.5× SSC (75 mM sodium chloride, 7.5 mM trisodium acetate, pH 7.0) at 42 °C. Cells were then fixed again with paraformaldehyde, washed in PBS, and incubated for 30 min at R/T with cy3-streptavidin (Jackson Immuno Research, PA) and secondary antibodies. Cells were stained with DAPI for nuclear labeling, and the cover slips were mounted on glass slides for confocal microscopy. Thirty PRRSV-infected MARC-145 cells were examined each experiment for quantification of positive cells.

2.10. VSIV-GFP bioassay

The IFN bioassay is described elsewhere (Kim et al., 2010). HeLa cells grown in 6-well plates were transfected with 2 μg of plasmid containing respective viral genes. At 24 h post-transfection, cells were stimulated with 1 μg of poly (I: C) by transfection and further incubated for 12 h. For PRRSV infections, MARC-145 cells in 12-well plates were infected at an MOI of 1. Supernatants were harvested from either PRRSV-infected or gene-transfected cells and serially diluted by 2-fold. For VSIV-GFP bioassay, MARC-145 cells were grown in 96-well plates and incubated for 24 h with 100 μl of each dilution of supernatants. Cells were then infected with 100 μl of VSIV-GFP of at 0.01 MOI and incubated for 16 h. Cells were fixed with 4% paraformaldehyde, and GFP expression was examined using an inverted fluorescence microscope (Nikon Eclipse TS100). The titers of IFN inhibition were determined as the highest dilution of supernatants inhibiting VSV-GFP replication.

3. Results

3.1. Impaired poly(A)+ RNA nuclear-cytoplasmic trafficking by PRRSV

Since two proteins (nsp1β and nsp11) of PRRSV have been reported to contain a nuclease activity (Nedialkova et al., 2009; Xue et al., 2010), a possible degradation of mRNA by PRRSV was initially postulated. Therefore, poly(A)+ RNA in PRRSV-infected cells was examined by in situ hybridization. As anticipated, poly(A)+ RNA was normally distributed in the both cytoplasm and nucleus in mock-infected cells (Fig. 1A, red). In contrast, red fluorescent intensities (FIs) were distinct in the nucleus in PRRSV-infected cells (Fig. 1A), indicating that PRRSV caused poly(A)+ RNA retention to the nucleus. Virus-infected cells were distinguished by staining with anti-nsp1β polyclonal antibody (pAb), and consistent with previous finding, nsp1β was distributed in the both cytoplasm and nucleus in infected cells (Fig. 1A). Since the PRRSV genome replication and transcription occur exclusively in the cytoplasm, the mRNAs in the nucleus are assumed to be cellular transcripts. To examine if the nuclear retention of mRNA by PRRSV was a common property for PRRSV, other strains of PRRSV representing the genotypes I and II were examined. Similar results were obtained for NVSL 97-7895 (FL12) (genotype II), VR2332 (genotype II), and the Lelystad virus (genotype I) (Fig. 1A), indicating that the nuclear accumulation of cellular mRNA is common for both genotypes of PRRSV.

To determine whether PRRSV-mediated host mRNA nuclear accumulation affects viral RNA translation, we examined the distribution of viral RNA by RT-qPCR using PRRSV N-gene specific primers. Most viral RNA was found in the cytoplasm (Fig. 1B). In addition to N transcripts, four cellular genes [*GADPH* (Glyceraldehyde 3-phosphate dehydrogenase), *DEPTOR* (DEP domain-containing mTOR-interacting protein), *NOL6* (nucleolar protein 6), *SH2* (src homology 2)] were randomly chosen and their mRNA nuclear/cytoplasmic ratios were determined by RT-qPCR and presented on the logarithmic scales (Fig. 1C). Compared to mock-infected cells, the nuclear/cytoplasmic ratios for *DEPTOR*, *NOL6*, and *SH2* transcripts were significantly increased to higher than 1 in PRRSV-infected cells, indicating that the majority of the mRNAs were localized in the nucleus during infection. On the contrary, the nuclear/cytoplasmic ratio for PRRSV transcripts was approximately 0.2, demonstrating that viral RNA was predominantly cytoplasmic. These results show that PRRSV infection imprisoned host mRNA to the nucleus without disrupting the cytoplasmic distribution of viral RNA.

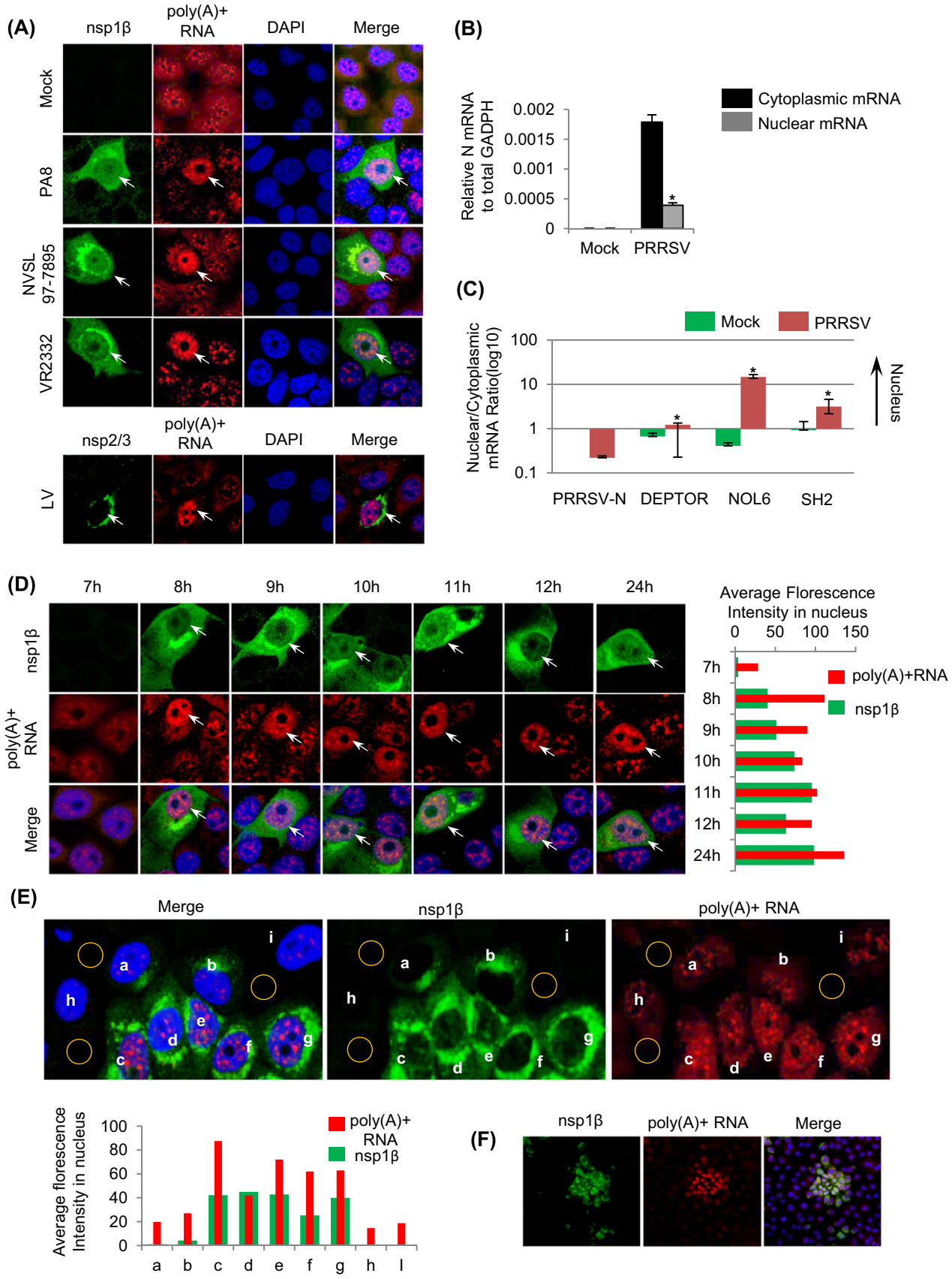

Fig. 1. Nuclear accumulation of poly(A)+ RNA mediated by PRRSV. (A) In situ hybridization (ISH) of cells infected with different strains of PRRSV. MARC-145 cells were infected by PRRSV for 24 h at a moi of 1. Arrows indicate PRRSV-infected cells. (B) RT-qPCR for nuclear and cytoplasmic PRRSV N RNA. Levels of cytoplasmic and nuclear mRNA were normalized with total *GAPDH* mRNA (combination of cytoplasmic and nuclear fractions). (C) Nuclear/cytoplasmic mRNA ratio. (N=3 from two independent experiments, mean ± SD; * different from mock, $P < 0.05$). (D) Distribution of cellular poly(A)+ RNA in PRRSV-infected cells at various times. A moi of 1 was used for infection. Arrows indicate PRRSV-infected cells. (E) Distribution of cellular poly(A)+ RNA in different cells at 24 h post-infection of PRRSV. (F) Low magnification images of the poly(A)+ RNA nuclear retention in PRRSV-infected cells.

The kinetics for PRRSV-mediated host mRNA nuclear accumulation was determined using the PA8 strain of PRRSV. The mRNA nuclear accumulation was detectable from 8 hpi until at least 24 hpi (Fig. 1D). FIs in the nucleus in virus-infected cells were quantified, and red FIs representing host mRNA and green FIs representing PRRSV-nsp1β both increased over time (Fig. 1D, right panel), suggesting that the host mRNA nuclear accumulation was associated with the nsp1β nuclear localization. To confirm this correlation, fluorescence analyses were conducted (Fig. 1E, individual cells are indicated by lower-case letters). Average nuclear FIs were determined for both host mRNA and nsp1β and normalized using average FIs in background (Fig. 1E, yellow circles). In comparison to uninfected cells (Fig. 1E, lower panel, lanes 'h' and 'I'), no increase of nuclear red FIs was observed in PRRSV-infected cells with no nuclear nsp1β (lanes 'a' and 'b'). By sharp contrast, nuclear red FIs were increased by 2–4 folds in cells with nuclear nsp1β (lanes 'c'–'g'), suggesting that the nuclear accumulation of host mRNA required nsp1β in the nucleus. PRRSV-infected cells showed significant host mRNA nuclear accumulation by 24 hpi (Fig. 1F).

3.2. mRNA nuclear accumulation is mediated by PRRSV nsp1β

The PRRSV replication occurs exclusively in the cytoplasm, but three viral proteins have been identified to localize specifically in the nucleus: nsp1α, nsp1β, and N proteins (Yoo, 2010). Thus, it was our interest to determine which viral proteins caused host mRNA nuclear accumulation. We included PIAS1 (protein inhibitor of activated STAT-1), which is a cellular nuclear protein, as a control (Fig. 2A). When these proteins were individually expressed, only cells expressing nsp1β exhibited host mRNA accumulation in the nucleus (Fig. 2A; arrows), indicating that the nsp1β protein was solely responsible for the nuclear accumulation of host mRNA. PIAS1 was normally localized in the nucleus as anticipated (Fig. 2A); however, no host mRNA accumulation was seen in these cells, indicating the specific nuclear accumulation of host mRNA.

To confirm the nuclear accumulation of host mRNA by PRRSV-nsp1β, nuclear mRNA levels for *DEPTOR*, *SH2*, and *NOL* were determined by RT-qPCR (Fig. 2B). Total mRNA was first determined by RT-qPCR from cells expressing mock (pXJ41; empty vector), nsp1α, nsp1β, or N genes. No significant changes in the total amount of chosen mRNA were seen for chosen genes in viral gene-transfected cells. To determine the amount of mRNA in the nucleus, the nuclear fraction was separated from the cytoplasmic fraction, followed by RT-qPCR. The total host mRNA in the nucleus was normalized using the total *GAPDH* mRNA of the nuclear and cytoplasmic fractions. In comparison to mock-control, the nuclear mRNAs in nsp1β-expressing cells were significantly increased for *DEPTOR*, *NOL6*, and *SH2* (Fig. 2B, lower panel). These results further confirmed that nsp1β caused host mRNA accumulation in the nucleus.

Since host mRNAs were not exported to the cytoplasm but rather accumulated in the nucleus by nsp1β, we next examined whether host protein synthesis was inhibited by nsp1β. The transfection efficiency in cells co-expressing nsp1β was first examined by co-transfecting *Renilla* reporter and nsp1β, followed by RT-qPCR for *Renilla*. No significant difference was seen compared to the control (data not shown). Then, each of the nsp1α, nsp1β, or N genes was co-transfected with the exogenous foreign gene GFP, and the amount of GFP protein was examined by Western blot. As indicated in Fig. 2C (asterisks), nsp1β caused a notable reduction of GFP expression. In contrast, the mock (pXJ41)-, nsp1α-, or N-gene did not cause the reduction of GFP expression. Taken together, it was concluded that PRRSV nsp1β imprisoned host mRNA in the nucleus, which may contribute to the reduction of host protein expression. Expression levels of the endogenous cellular protein DEPTOR were also examined using anti-DEPTOR antibody, and DEPTOR was found to decrease in nsp1β-expressing cells. (Fig. 2D), confirming the reduction of host protein expression by nsp1β.

3.3. Poly(A)+ RNA nuclear export by individual SAP mutants

The PRRSV nsp1β protein contains a papain-like proteinase domain (PLP1β) and a nuclease motif. Further analysis of the nsp1β sequence revealed a motif at residues 123–138 resembling the previously defined SAP domain for protein-DNA interactions (Abraham and Sarnow, 2011). The motif of 124-KxLQxxLxxxGL-135 in PRRSV-nsp1β meets the SAP consensus motif in the first α-helix, xPLBxxHxxBxH, where P, B, and H indicate polar, bulky, and hydrophobic residues, respectively. The leader proteinase (Lpro) protein of foot-and-mouth disease virus (FMDV) contains a SAP motif, and mutations in the first α-helix of the SAP motif were sufficient to subvert its function (de los Santos et al., 2009). Hence, we hypothesized that this conserved sequence motif might function similar to SAP, and accordingly a total of seven single mutations were individually introduced to the SAP motif of PRRSV-nsp1β. To examine whether the SAP domain was associated with nsp1β-mediated host mRNA nuclear accumulation, the ability of SAP mutants for host mRNA nuclear export was individually examined by in situ hybridization (Fig. 3A). The nuclear accumulation of poly(A)+ RNA was evident for wild-type nsp1β and two mutants K124A and G134A, whereas no accumulation was observed for the rest of mutants. The average nuclear FIs were determined for red fluorescence and green fluorescence representing poly(A)+ RNA and nsp1β, respectively. Wild-type nsp1β, K124A, and G134A resulted in the strong poly(A)+ RNA and nsp1β in the nucleus, while the mutants L126, R129, L130A, and L135A showed the weak FIs. For R128A, poly(A)+ RNA were weak but nsp1β were strong in the nucleus, suggesting that the residue R128 was essential for the nuclear retention of poly(A)+ RNA but nonessential for the nsp1β nuclear localization (Fig. 3B). To examine the relative amounts of host mRNA in the nucleus of the mutant nsp1β-expressing cells, the *DEPTOR*, *NOL6*, and *SH2* genes were chosen as cellular genes for RT-qPCR, and R128A and L135A were chosen as representative viral mutants (Fig. 3C). No significant fold-changes were seen in the total host mRNA by nsp1β and its mutants (Fig. 3C, upper panel), but two SAP mutants R128A and L135A reduced the amounts of DEPTOR, NOL6, and SH2 mRNAs when compared to nsp1β (Fig. 3C, lower panel), further indicating that the SAP motif was essential to retain host mRNAs in the nucleus.

3.4. SAP motif in PRRSV-nsp1β and its biological activities

Suppression of host protein synthesis by SAP mutants was next analyzed. Endogenous DEPTOR protein expression was examined by Western blot. Wild-type nsp1β and the G134A mutant suppressed DEPTOR expression, but L126A and L135A did not reduce the expression (Fig. 4A). The *Renilla* reporter system and the GFP expression were used to determine the levels of two different ectopic gene expressions. While nsp1β caused the reduction of *Renilla* expression, all other mutants, with exceptions of K124A and G134A, were unable to suppress *Renilla* expression (Fig. 4B). When expression levels of GFP were examined in nsp1β-expressing and SAP mutants-expressing cells, all other mutants, with an exception of wild-type nsp1β, K124A, and G134A, did not inhibit GFP expression (Fig. 4C), which was consistent with the results from *Renilla* expression. The experiments using two exogenous genes indicate that the SAP motif is required for nsp1β to suppress gene expression.

The substitution of hydrophobic residues in the SAP motif FMDV L^{pro} was shown to alter its subcellular localization (de los Santos et al., 2009). Thus, it was of interest to examine whether the SAP mutations of PRRSV nsp1β also altered their cellular distributions. When each of the mutants were expressed in cells, the nuclear distribution was predominant for K124A, R128A, and G134A, and their distribution patterns were indistinguishable from that of wild-type nsp1β (Fig. 4D). By contrast, the distribution of L126A, R129A, L130A, and L135A became exclusively cytoplasmic. The nuclear and cytoplasmic distribu-

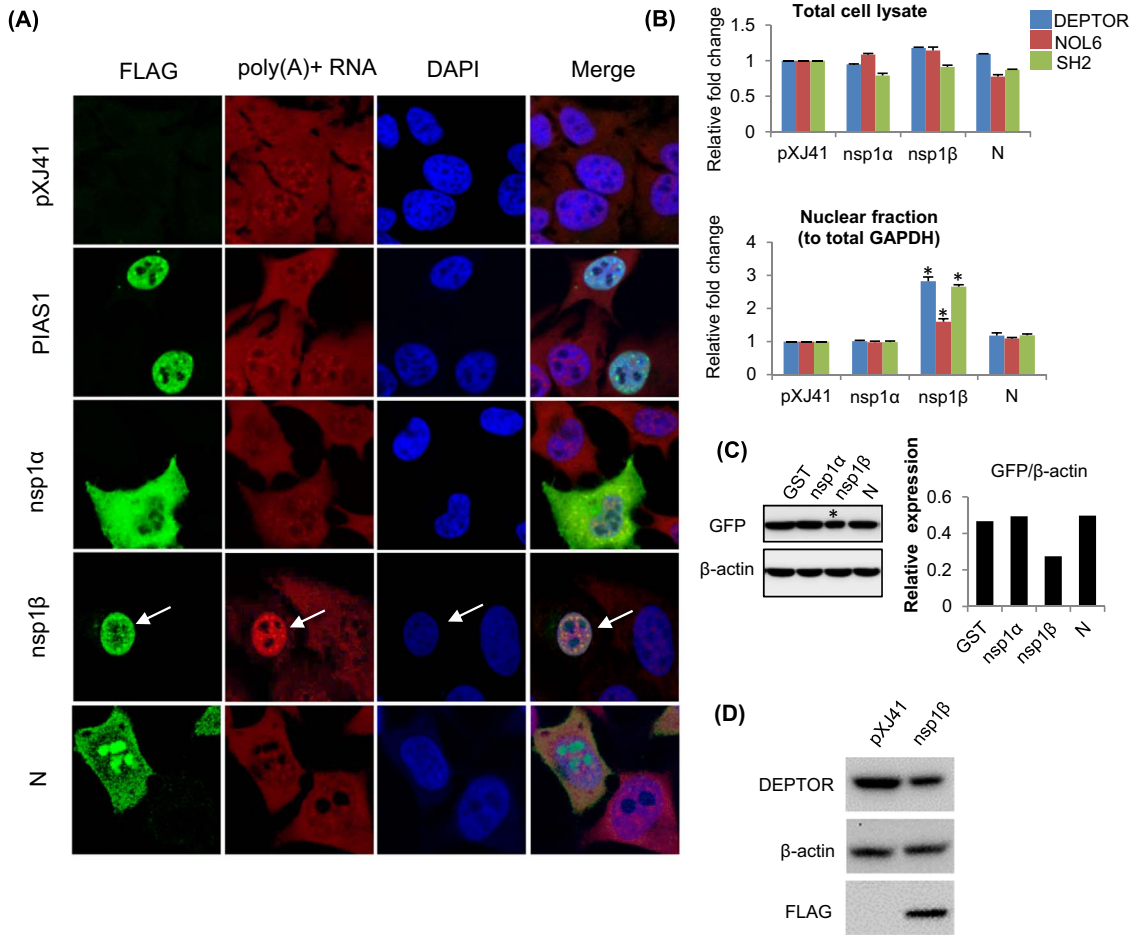

Fig. 2. PRRSV-nsp1β-mediated nuclear mRNA retention. (A) Distribution of poly(A)+ RNA in HeLa cells expressing PIAS1, nsp1α, nsp1β, and N. Cellular localization of individual gene products (green) and poly(A)+ RNA (red) were examined by confocal microscopy (Zeiss). Arrows indicate nsp1β gene-transfected cells. (B) RT-qPCR for *DEPTOR*, *NOL6*, and *SH2* in gene-transfected cells. Total mRNA and nuclear mRNA were normalized with total *GAPDH*. Gene expressions in pXJ41 were used to calculate relative fold change (N=3 from two independent experiments, mean ± SD; *different from pXJ41, $P < 0.05$). (C) Co-expression of an exogenous foreign gene (GFP) with nsp1β. GFP expressions were quantified and normalized using β-actin. (D) Co-expression of a endogenous cellular gene (DEPTOR) with nsp1β.

tions of nsp1β SAP mutants were confirmed by cell fractionation and Western blotting (Fig. 4E). HSP90 and PARP served as the cytosolic and nuclear protein controls, respectively, and remained in their respective compartment, excluding the possible cross-contamination during cell fractionation.

3.5. Generation of SAP mutant PRRS viruses and their biological characteristics

Since the SAP function of nsp1β was demonstrated by ectopic gene expression, it was necessary to verify the function in the context of virus infection. To do this, seven SAP mutant viruses with respect to K124A, L126A, G134A, L135A, R128A, R129A, and L130A were generated by reverse genetics using infectious clones, and designated vK124A, vL126A, vG134A, vL135A, vR128A, vR129A, and vL130A, respectively. After transfection of MARC-145 cells with individual full-length genomic clones, viral infectivity was determined by IFA and Western blot for N protein expression. Of seven mutant constructs, vR128A, vR129A, and vL130A appeared to be non-available, and four mutants vK124A, vL126A, vG134A, and vL135A were obtained. The reconstituted PRRSV mutants were amplified in MARC-145 cells by five passages and their genetic stability was determined by sequencing. Respective mutations appeared to be stable in cell culture. SAP mutant viruses of vK124A, vL126A, vG134A, and vL135A were titrated using each of P1, P2, and P3 passages, and their titers of P3 passages reached 10^4, $10^{3.67}$, $10^{5.83}$, and $10^{3.83}$ per ml of $TCID_{50}$, respectively. The titer of the parental virus reconstituted from the FL13 wild-type infectious clone was determined to be 10^5/ml $TCID_{50}$ (Fig. 5A). The multi-step growth kinetics revealed that the mutant viruses vL126A and vL135A exhibited decreased growth rates with the peak titers of approximately 100-fold lower compared to that of wild-type PRRSV vFL13 (Fig. 5B). The titers of vK124A and vG134A were similar to that of FL13 (Fig. 5B). The plaque size of vL126A and vL135A was reduced significantly, compared to the vFL13 plaques (Fig. 5C). All together, these results show that the SAP motif in nsp1β is crucial for PRRSV replication.

In Fig. 4, we showed the cellular localization of SAP mutant nsp1β in ectopically expressing cells and wanted to validate the findings in the SAP mutant virus-infected cells (Fig. 5D). MARC-145 cells were infected with each of viable vK124A, vL126A, vG134A, or vL135A, and infected cells were co-stained with N- and nsp1β-specific antibodies. As with wild-type vFL13-infected cells, vK124A and vG134A-infected cells showed nsp1β staining in the nucleus, whereas vL126A and vL135A did not cause the nsp1β nuclear staining, which was consistent with the results of the nsp1β-gene-transfection. The FIs were calculated, and the average nuclear red FIs indicating nsp1β were above 80, indicating strong FIs for vFL13, vK124A, and vG134A (Fig. 5D, right panel). The FIs for each mutants were confirmed by cell fractionation and Western blot analyses (Fig. 5E, upper panel). In contrast, vL126A and vL135A showed limited amounts of nsp1β in the nucleus (Fig. 5E, upper panel), further confirming that the SAP domain was important for the nsp1β nuclear localization. The production of

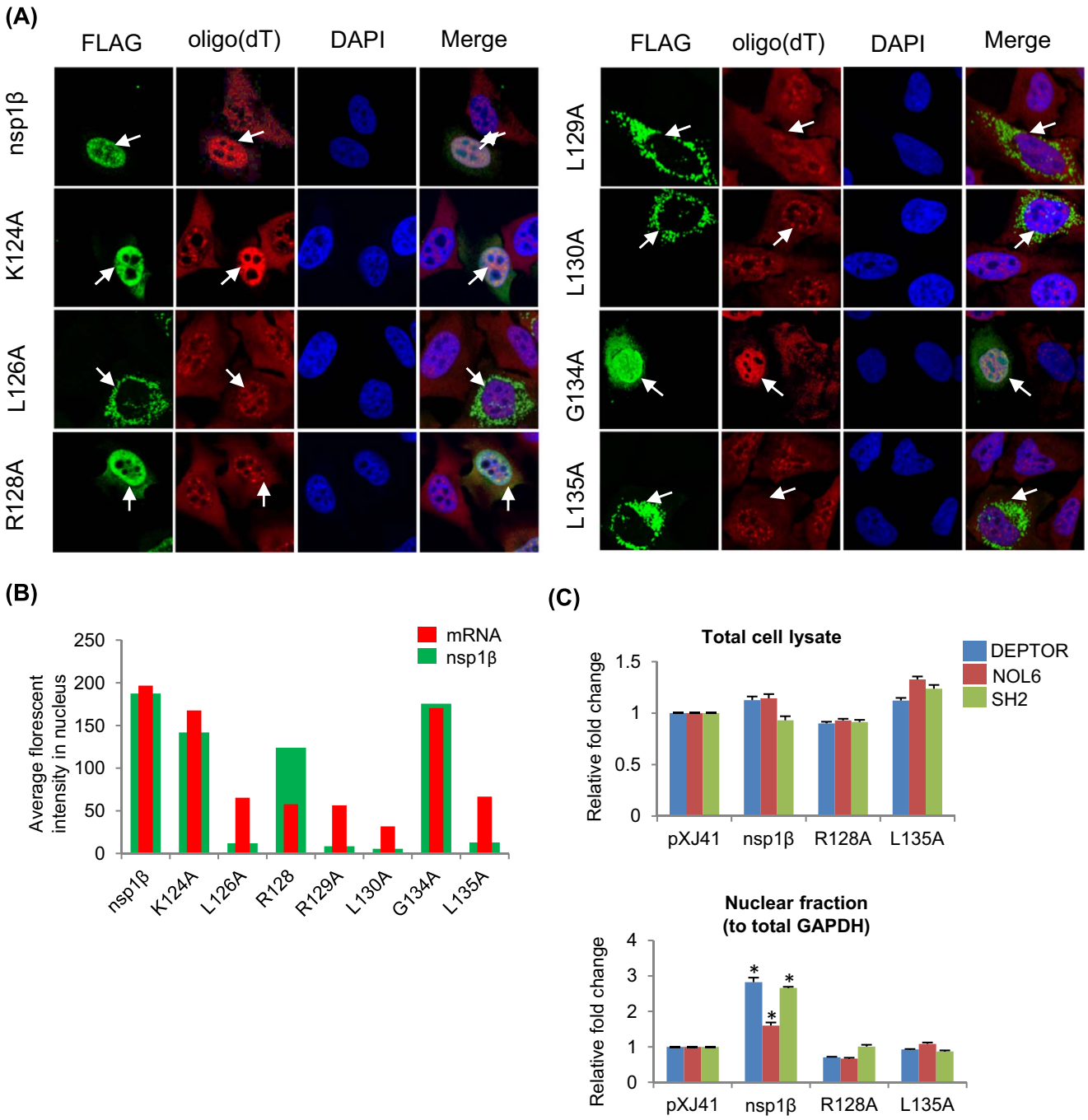

Fig. 3. (A) and (B). Nuclear retention of poly(A)+ RNA in SAP-mutant nsp1β-expressing cells. Arrows indicate gene-transfected cells (C) RT-qPCR for *DEPTOR*, *NOL6*, and *SH2* in cells expressing SAP mutants. Total mRNA and nuclear mRNA were normalized with total *GAPDH*. Gene expressions in pXJ41 were used to calculate relative fold change (N=3 from two independent experiments, mean ± SD; * different from pXJ41, $P < 0.05$).

nsp1β was examined by Western blot using the total cell lysate after virus infection, and the production of nsp1β was not impaired by SAP mutations (Fig 5E).

3.6. mRNA nuclear export in cells with SAP mutants infection

Since the exclusive cytoplasmic distribution of nsp1β was seen for vL126A and vL135A infections, it was of interest to examine whether host mRNAs were retained in the nucleus in vL126A-infected or vL135A-infected cells. MARC-145 cells were infected with each of SAP mutant viruses for 24 h, and host mRNA hybridization was conducted using an oligo(dT) probe. Host mRNA nuclear retention was found to be significant in cells infected with vK124A and vG134A as well as wild-type FL13, but was not seen in cells infected with vL126A and vL135A (Fig. 6A). Since vL126A and vL135A did not block the host mRNA export from the nucleus, it was assumed that these two mutant viruses were unable to suppress the IFN production. To confirm this premise, IFN production was examined by IFN-β-Luc reporter assay as described previously (Li et al., 2013). Parental PRRSV vFL13 and vG134A significantly inhibited the luciferase activity when compared to mock-infected cells. In contrast, the L126A and L135A mutants were no longer able to suppress the reporter activity, demonstrating inability of IFN suppression by L126A and L135A (Fig. 6B).

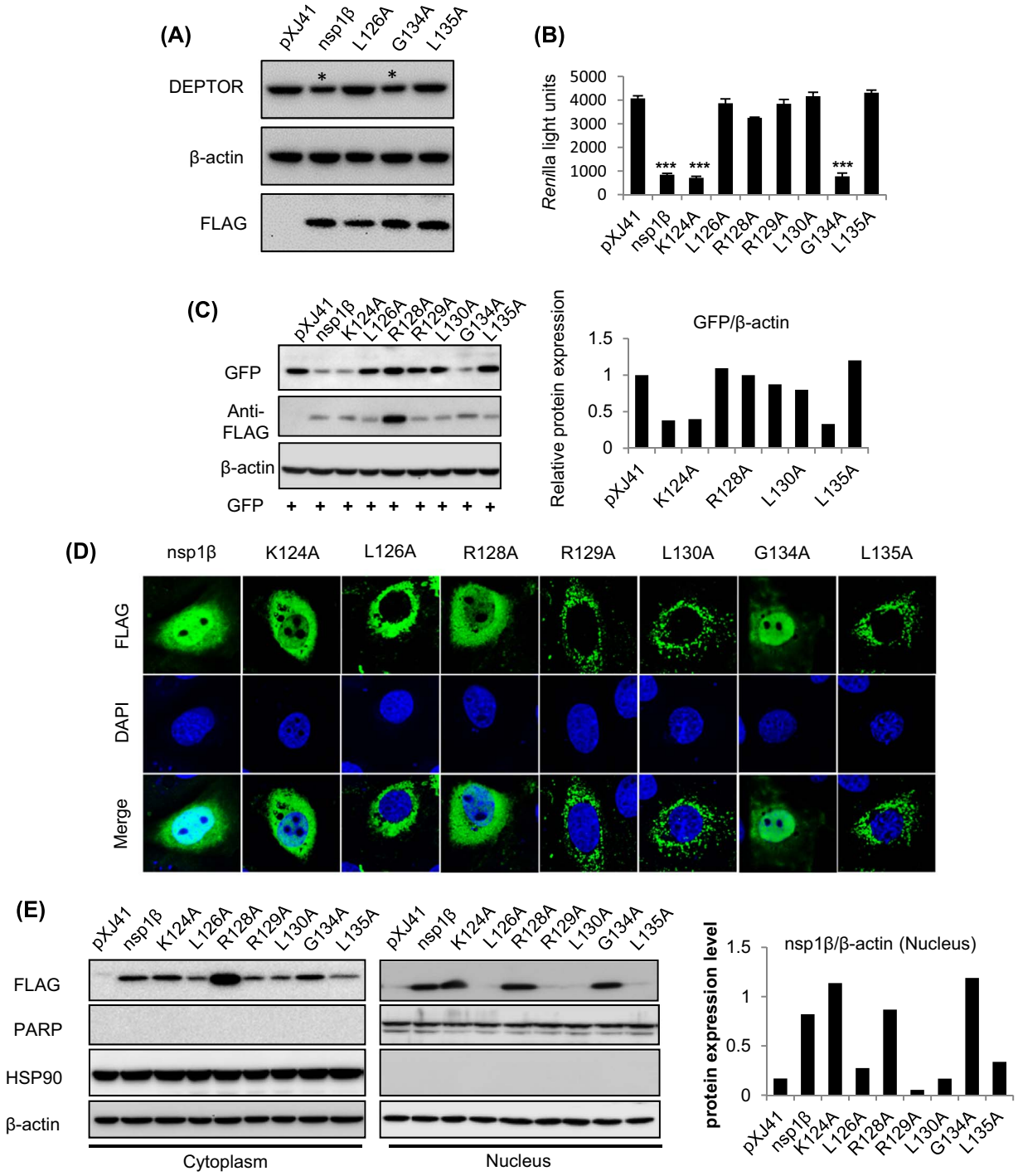

Fig. 4. Biological activities of SAP mutants. (A) Reduction of DEPTOR expression in cells expressing nsp1β and its mutants. DEPTOR expression was normalized using β-actin. HeLa cells were co-transfected with the *Renilla* reporter pRL-TK (B) or GFP-expressing pEGFP-N1 (C), along with individual SAP mutants. (N=3 from three independent experiments, mean ± SD; * different from pXJ41; *, $P < 0.05$; **, $P < 0.01$; ***, $P < 0.001$). (D) Cellular distribution of SAP mutant proteins in MARC-145 cells. (E) Nuclear localization of SAP mutants. MARC-145 cells expressing individual SAP mutants were fractionated followed by Western blot. X-axis represents individual SAP mutants. Y-axis represents relative levels of nsp1β protein expression in the nucleus normalized using the nuclear β-actin as a control.

3.7. SAP domain of nsp1β and suppression of innate immune signaling

PRRSV nsp1β has been shown to participate in the suppression of IFN production and signaling. Hence, it was of interest to examine whether the SAP domain of nsp1β was involved in the IFN suppression. The SAP mutants were expressed in cells by gene transfection and the IFN production was induced by poly(IC) stimulation followed by IFN reporter assays (Fig. 7A). The IFN production was high when stimulated by poly(IC) treatment as anticipated in pXJ41 mock-transfected cells, or the unrelated GST (glutathione S-transferase)-expressing cells. In contrast, the inhibition of IFN production was evident for wild-type nsp1β-expressing cells. As with nsp1β, the mutants K124A, R128, and G134 also inhibited the IFN promoter activity. Interestingly however, L126A, R129A, L130A, and L135A did not inhibit the IFN induction (Fig. 7A), and these were the mutants that did not accumulate host mRNA in the nucleus. These observations indicate the positive correlation of SAP domain with the IFN suppression. R128A appeared

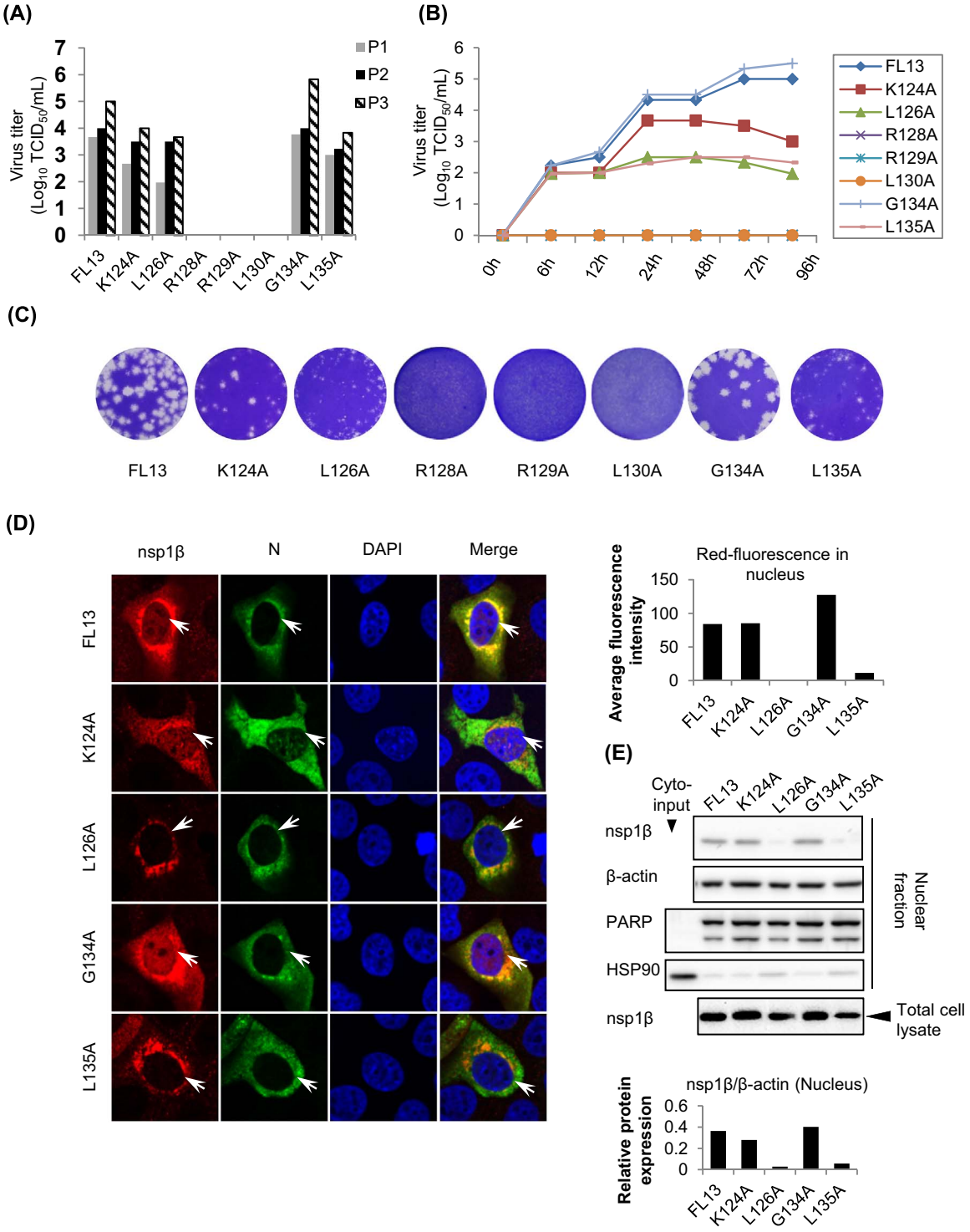

Fig. 5. Growth kinetics of SAP mutant PRRSV in MARC-145 cells. (A) Titers of wild-type and SAP mutant viruses during the first three passages. The titers are expressed as $\log^{10}$ $TCID_{50}$/ml. The culture supernatants from DNA-transfected cells were designated passage-1. (B) Growth curves for FL13-WT and SAP mutant viruses. Cells were infected at a moi of 0.1 with the passage-3 preparation of indicated virus in duplicate. Samples were collected at the indicated times, and virus titers were determined. The results are expressed as mean values from two independent experiments, and error bars represent standard errors of mean values from two experiments. (C) Plaque morphology of SAP mutant viruses. (D) Subcellular localizations of nsp1β in SAP mutant virus-infected cells. (E) MARC-145 cells infected with FL13-WT or SAP mutant viruses were fractionated to obtain nucleus, and the nuclear nsp1β level was determined by Western-blot using anti-PRRSV-nsp1β rabbit antiserum. The expression of nsp1β was normalized using β-actin.

to cause a moderate level of suppression. To further demonstrate the function of SAP for IFN suppression, VSIV-GFP bioassay was conducted for individual SAP mutants. The inhibition titers for L126A, R129A, L130A, and L135A were 1:16, and these titers were comparable to those of two negative controls, the empty vector control and the GST control (Fig. 7B). The inhibition titer for nsp1β was 1:1. A representative proinflammatory cytokine TNF-α was also examined for SAP mutants after stimulation with LPS (Fig. 7C). The TNF-α promoter activity was significantly suppressed by nsp1β, K124A, and G134A, whereas no suppression was observed for L126A, R129A, L130A, and L135A (Fig. 7C). These data were consistent with the results for IFN suppression and supportive that the SAP domain of

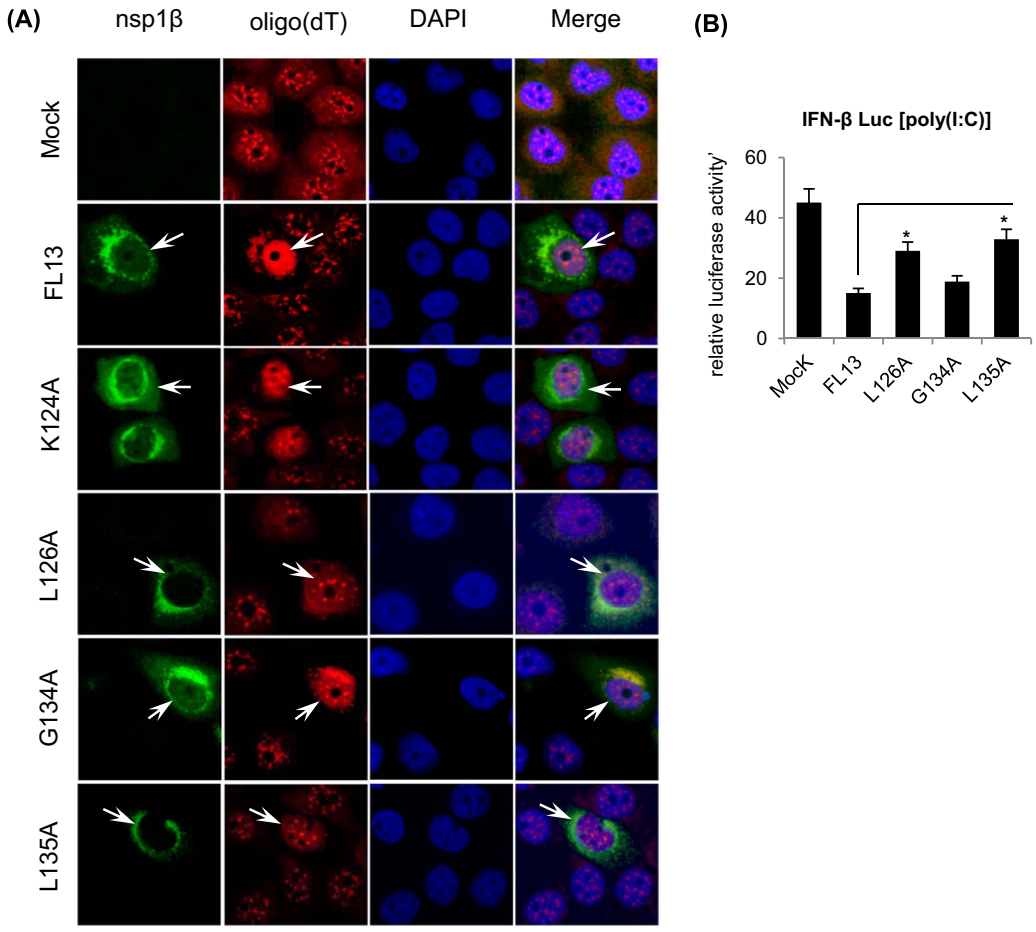

Fig. 6. Nuclear mRNA imprisonment by SAP mutants. (A) PRRSV vFL13, vK124A, vL126A, vG134A and vL135A were used to infect MARC-145 cells at a moi of 0.1 for 24 h. White arrows indicate PRRSV-infected cells. (B) Regulation of type I IFN production by SAP mutant viruses. (N=3 from three independent experiments, mean ± SD; * different from vFL13, $P < 0.05$).

nsp1β played a major role for innate immune signaling induced by PRRSV.

PRRSV nsp1β has also previously been shown to suppress the JAK-STAT signaling pathway (Patel et al., 2010). Thus, we examined whether the SAP domain was involved in the nsp1β-mediated suppression of JAK-STAT pathway (Fig. 7D). For this experiment, ISRE-dependent luciferase assay was conducted in cells expressing individual SAP mutants. As with wild-type nsp1β, the mutants K124A and G134A suppressed the ISRE-Luc activity significantly and partially for R128A (Fig. 7D). In contrast, L126A, R129A, L130A, and L135A were unable to suppress the ISRE-mediated luciferase expression. To further confirm the ISRE suppression, the expression of ISG15, an ISRE-dependent IFN-stimulated gene (ISGs) products, was examined by Western blot using two SAP mutants L126A and R129A (Fig. 7E). While the reduction of ISG15 was evident for nsp1β (lane 3, asterisk), L126A and R128A did not inhibit the expression of ISG15. These results confirmed the essential role of SAP domain for suppression of innate immune responses by nsp1β.

3.8. Retention of host mRNA by nsp1 in the family Arteriviridae

Since PRRSV nsp1β caused host mRNA accumulation in the nucleus, it was plausible that nsp1 of other arteriviruses might possess a similar function. To examine this possibility, HeLa cells were co-transfected with the LDV-nsp1α- or LDV-nsp1b-genes, and for SHFV, SHFV-nsp1α-, SHFV-nsp1b-, and SHFV-nsp1γ-genes were transfected along with the *Renilla* luciferase reporter, followed by reporter assays. For EAV, nsp1 is uncleaved and remains as a single protein, thus, the full-length nsp1 gene was transfected for EAV. In cells expressing LDV-nsp1β and SHFV-nsp1β, *Renilla* expression was reduced to the level of PRRSV-nsp1β (Fig. 8A). For other constructs, no significant reduction was observed. Consistent with this finding, poly(A)+ RNA accumulation was evident in the nucleus of cells expressing PRRSV-nsp1β, LDV-nsp1β, and SHFV-nsp1β (Fig. 8B). The average red FIs in the nucleus were calculated, and LDV-nsp1β and SHFV-nsp1β were shown to have similar intensities to that of PRRSV-nsp1β (Fig. 8C). 96%, 94%, and 90% of cells showed nuclear poly(A)+ RNA retention for PRRSV-nsp1β, LDV-nsp1β, and SHFV-nsp1β, respectively (Fig. 8D). Unexpectedly, no retention of host mRNA was observed for EAV-nsp1 (Fig. 8B), suggesting that EAV nsp1 does not contain this function. These results indicate that the imprisonment of host mRNA in the nucleus by nsp1 is common for PRRSV, LDV, and SHFV, but EAV.

4. Discussion

As with many other plus-strand RNA viruses, arterivirus genomes are 5′-capped (Snijder et al., 2013), and thus, a cap-dependent translation is essential for viral protein production. In the present study, we have described that PRRSV blocks the nuclear export of host mRNAs to the cytoplasm and accumulates them in the nucleus (Fig. 1). This is a novel finding for viruses in the order of Nidovirales. The virus-mediated nuclear imprisonment of host mRNAs makes them difficult to access the cytoplasm for translation, while the viral genomic RNA and subgenomic mRNAs can effectively recruit ribosomes for efficient translation with less competitions with host mRNAs. A small amount

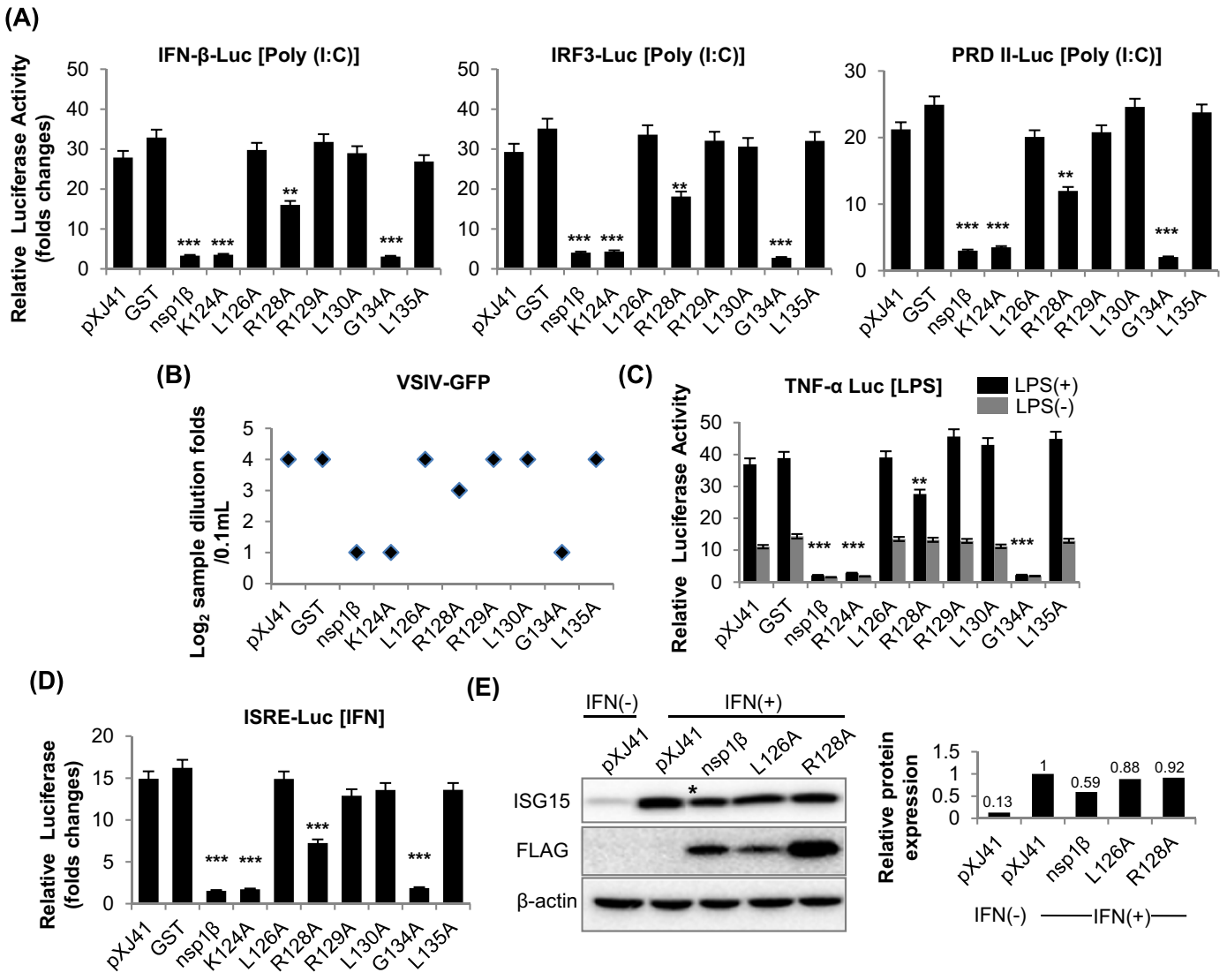

Fig. 7. Suppressions of innate immune signaling by SAP mutants. Regulation of type I IFN production (A), TNF-α promoter activity (C), and ISRE-promoter activity (D) by SAP mutants. Relative luciferase activities were calculated by normalizing the firefly luciferase to *Renilla* luciferase activities. (B) IFN bioassay using VSIV-GFP. (E) The expression of IFN-stimulated gene 15 (ISG15) was analyzed in cells transfected with SAP constructs after incubating with IFN (1000 units/ml) for 2 h. ISG15 level was normalized with β-actin. (N=3 from three independent experiments, mean ± SD; * different from pXJ41; *, $P < 0.05$; **, $P < 0.01$; ***, $P < 0.001$).

of viral RNA is detected by oligo(dT) probe, and this is probably due to the binding of viral RNA with nsp1β protein (Xue et al., 2010), resulting in the nuclear transport of viral RNA by piggyback riding on the nsp1β. The host mRNA nuclear retention is observed for both genotypes (types I and II) of PRRSV, and LDV and SHFV, suggesting that this strategy is extensively utilized by PRRSV and by other member viruses in the family *Arteriviridae* with an exception of EAV. Host mRNA nuclear accumulation is not observed by EAV nsp1, despite EAV nsp1 being a nuclear protein, which suggests a different mechanism for EAV nsp1 to mediate IFN suppression.

The nuclear localization of PRRSV N protein relies on the specific nuclear localization signal (NLS), and the NLS of N has been shown to be a virulence factor of PRRSV (Pei et al., 2008). The nsp1α in the nucleus participates in the CREB-binding protein degradation (Han et al., 2013). It has been noted that nsp1β protein is distributed exclusively in the nucleus in gene-transfected cells but is distributed both in the nucleus and cytoplasm in virus-infected cells. The reason for such a difference is unclear, but may be due to the interaction of nsp1β with nsp1 to mediate nsp2TF frameshifting during virus infection, whereas in gene-transfected cells, such an interaction with nsp2 is absent. We have shown that the host mRNA nuclear accumulation is associated with the nuclear distribution of nsp1β. In PRRSV-infected cells, host mRNA nuclear accumulation is significantly in concert with the nsp1β nuclear staining (Fig. 1D). According to the kinetic studies, host mRNA accumulation is detectable as early as 8 h of infection, which is consistent with the first appearance of nsp1β in the nucleus (Fig. 1D).

All subunits of nsp1 of arteriviruses are able to suppress IFN production. As one of the suppression mechanisms, PRRSV-nsp1α, LDV-nsp1α, and SHFV-nsp1γ degrade the CREB-binding protein in the nucleus (Han et al., 2014), and for SHFV-nsp1αβ, the domain responsible for IFN suppression has been mapped to the nsp1β portion (Han and Yoo, 2014). PRRSV-nsp1β is a multifunctional protein inhibiting various signaling pathways including the IFN production, IFN signaling, and TNF-α production (Beura et al., 2010; Patel et al., 2010; Song et al., 2010). It is tempting to assume that such inhibitions by nsp1β may be due to the inhibition of nsp1β-mediated host mRNA nuclear export.

A SAP motif is found in some of host cell nuclear proteins besides PRRSV nsp1β, including the scaffold attachment factors A and B (SAF-

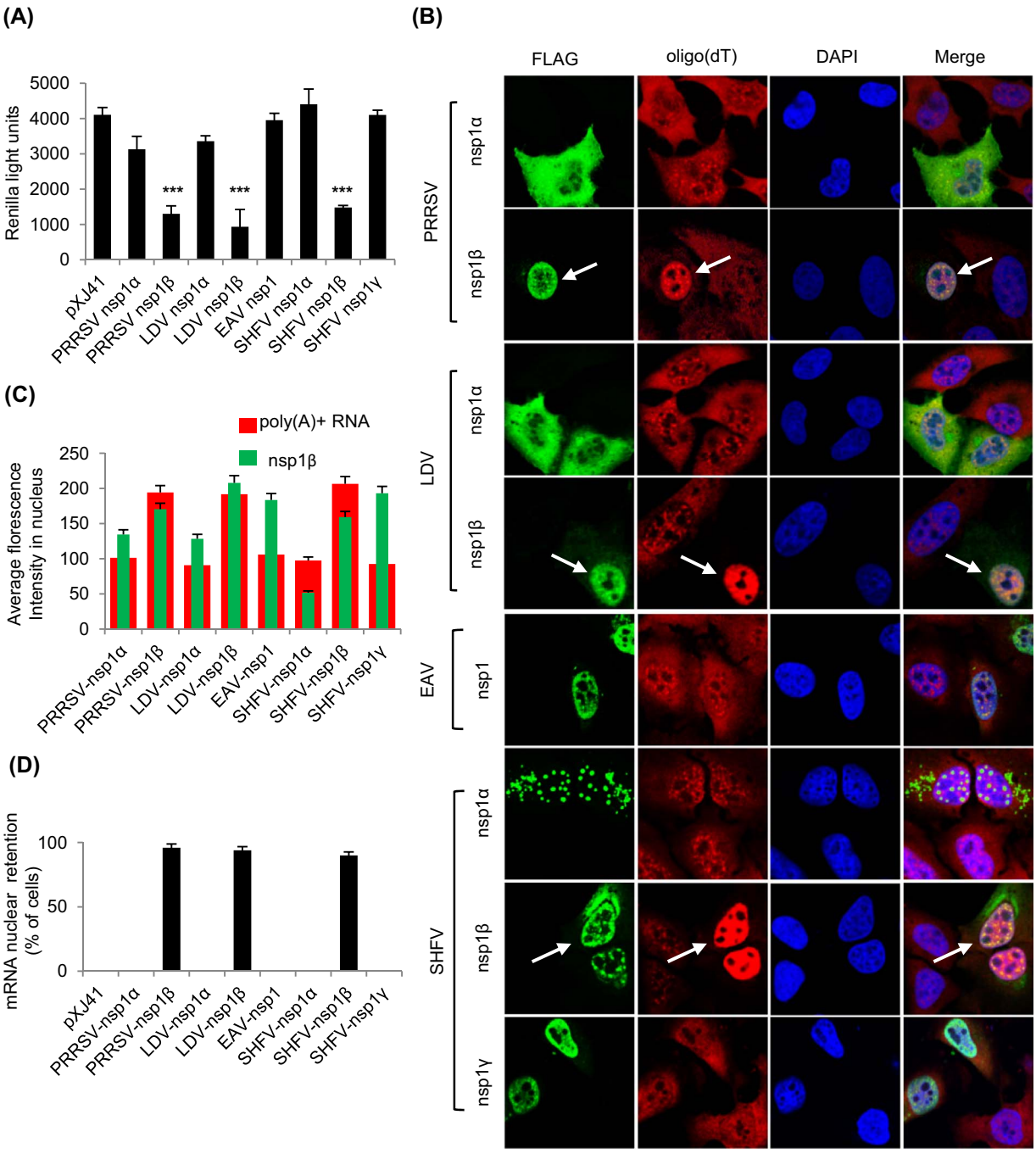

Fig. 8. Poly(A)+ RNA nuclear retention by nsp1 subunits in arteriviruses. (A) HeLa cells were co-transfected with individual constructs expressing arterivirus nsp1 subunits together with the *Renilla* reporter. (N=3 from three independent experiments, mean ± SD; *different from pXJ41; *, $P < 0.05$; **, $P < 0.01$; ***, $P < 0.001$) (B) and (C). ISH in cells expressing arterivirus nsp1 subunits. Arrows indicate gene-transfected cells with mRNA nuclear retention. (D) The percentage of cells showing significant nuclear poly(A)+ RNA retention was calculated using the following formula; (Number of cells showing significant nuclear poly(A)+ RNA staining intensity compared to the control nuclear poly(A)+ RNA staining intensity out of 50 nsp1-expressing cells/(50 cells expressing nsp1)×100.

A and -B), PIAS, and myocardia (Aravind and Koonin, 2000; Okubo et al., 2004). The SAP motif is essential for binding to AT-rich DNA sequences present in scaffold-attachment region/matrix-attachment region (SAR/MAR) (Aravind and Koonin, 2000). The signature motif of LxxLL in the N-terminal region of SAP domain of PIAS leads to the inhibition of STAT1-dependent transcription, whereas a SAP mutant of PIAS does not inhibit type I IFN transcription (Kubota et al., 2011; Liu et al., 2001). A SAP domain is also found in L^{pro} of foot-and-mouse disease virus (FMDV), and mutations introduced in the conserved SAP motif prevent the nuclear localization of L^{pro} and degradation of NF-κB (de los Santos et al., 2009). Remarkably, a SAP-mutant FMDV was attenuated and did not cause clinical signs, and the cattle immunized with the SAP-mutant FMDV developed a strong neutralizing antibody response (Segundo et al., 2012). The composition of SAP sequence identified in PRRSV nsp1β meets the SAP consensus motif identified in the cellular proteins, and three hydrophobic residues of L126, L130, and L135 are highly maintained in PRRSV nsp1β.

A highly conserved sequence of $_{123}$-GKYLQRRLQ-$_{131}$ has been reported in PRRSV nsp1β, which is partially overlapped with the SAP motif, and the K124A/R128A mutant impairs nsp1β-mediated IFN suppression (Li et al., 2013). In our study, the SAP mutants L126A, R129A, L130A, and L135A also resulted in the reversion of IFN

suppression but the molecular basis seems to differ from that of K124A/R128A mutation. Host mRNA nuclear accumulation was not observed in cells expressing mutants, except R128A which still confers the host mRNA nuclear accumulation. In contrast, the mutants L126A, R129A, L130A, and L135A remained in the cytoplasm and were co-localized with a mitochondria marker protein, suggesting the hydrophobic residues in the SAP motif may be essential for nuclear translocation of PRRSV nsp1β. Surprisingly, the subcellular distribution pattern of R129A was identical to those of leucine mutants (Fig. 4). PRRSV nsp1β suppressed the innate immune responses (Han and Yoo, 2014), and the SAP mutants L126A, R129A, L130A, and L135A failed to inhibit the IFN production, IFN signaling, and TNF-α induction plus host mRNA nuclear accumulation (Figs. 6 and 7), demonstrating that nsp1β-mediated host mRNA nuclear retention is closely involved in the nsp1β-regulated innate immunity. The mutant R128A showed partial reversion and this mutant did not imprison host mRNA in the nucleus (Figs. 6 and 7), suggesting that host mRNA nuclear accumulation is not the only mechanism for nsp1β-mediated innate suppression.

The leucine residues within the SAP motif are essential for host mRNA nuclear retention, and subsequently two viable mutants vL126A and vL135A were generated using infectious clones (Fig. 5). For these mutant viruses, the growth was impaired when compared to the parental vFL13 and vG134A (Fig. 5). nsp1β was retained in the cytoplasm when infected with vL126A and vL135A viruses, and no host mRNA nuclear accumulation was observed, which is consistent with the findings in gene-transfected cells (Fig. 3). Accordingly, the degree of IFN suppression was reduced, indicating that host mRNA nuclear retention contributes to host innate immune gene expression. nsp1β functions as a trans-activator to induce −1/−2 frameshifting in the nsp2 region of PRRSV and to produce nsp2TF and nsp2N (Li et al., 2014). The SAP leucine residues are in close proximity to the mutated residues of nsp1β-knock-out virus (1βKO) which fails to express nsp2TF and nsp2N, and thus it is plausible that the SAP mutant viruses vL126A and vL135A may be unable to produce nsp2TF and nsp2N.

In summary, we have shown that PRRSV infection causes host cell mRNA retention to the nucleus. PRRSV nsp1β is the viral protein responsible for the host mRNA nuclear imprisonment. The SAP motif in the nsp1β protein is essential for the nsp1β subcellular distribution, host mRNA nuclear retention, and modulation of host innate immune signaling.

Acknowledgements

This project was supported by the Cooperative State Research Service, U.S. Department of Agriculture (USDA), under Project no. ILLU-888-353, and Agriculture and Food Research Initiative (AFRI) Competitive Grant no. 2013-67015-21243 from USDA-National Institute of Food and Agriculture (NIFA).

Appendix A. Supporting information

Supplementary data associated with this article can be found in the online version at doi:10.1016/j.virol.2017.02.004.

References

Abraham, T.M., Sarnow, P., 2011. RNA virus harnesses microRNAs to seize host translation control. Cell Host Microbes 9, 5–7.
Aravind, L., Koonin, E.V., 2000. SAP – a putative DNA-binding motif involved in chromosomal organization. Trends Biochem. Sci. 25, 112–114.
Benfield, D.A., Nelson, E., Collins, J.E., Harris, L., Goyal, S.M., Robison, D., Christianson, W.T., Morrison, R.B., Gorcyca, D., Chladek, D., 1992. Characterization of swine infertility and respiratory syndrome (SIRS) virus (isolate ATCC VR-2332). J. Vet. Diagn. Invest 4, 127–133.
Beura, L.K., Sarkar, S.N., Kwon, B., Subramaniam, S., Jones, C., Pattnaik, A.K., Osorio, F.A., 2010. Porcine reproductive and respiratory syndrome virus nonstructural protein 1beta modulates host innate immune response by antagonizing IRF3 activation. J. Virol. 84, 1574–1584.
Chakraborty, P., Satterly, N., Fontoura, B.M., 2006. Nuclear export assays for poly(A) RNAs. Methods 39, 363–369.
Dalton, K.P., Rose, J.K., 2001. Vesicular stomatitis virus glycoprotein containing the entire green fluorescent protein on its cytoplasmic domain is incorporated efficiently into virus particles. Virology 279, 414–421.
de los Santos, T., Segundo, F.D., Zhu, J., Koster, M., Dias, C.C., Grubman, M.J., 2009. A conserved domain in the leader proteinase of foot-and-mouth disease virus is required for proper subcellular localization and function. J. Virol. 83, 1800–1810.
Ehrhardt, C., Kardinal, C., Wurzer, W.J., Wolff, T., von Eichel-Streiber, C., Pleschka, S., Planz, O., Ludwig, S., 2004. Rac1 and PAK1 are upstream of IKK-epsilon and TBK-1 in the viral activation of interferon regulatory factor-3. FEBS Lett. 567, 230–238.
Fang, Y., Treffers, E.E., Li, Y., Tas, A., Sun, Z., van der Meer, Y., de Ru, A.H., van Veelen, P.A., Atkins, J.F., Snijder, E.J., Firth, A.E., 2012. Efficient -2 frameshifting by mammalian ribosomes to synthesize an additional arterivirus protein. Proc. Natl. Acad. Sci. USA 109, E2920–E2928.
Firth, A.E., Zevenhoven-Dobbe, J.C., Wills, N.M., Go, Y.Y., Balasuriya, U.B., Atkins, J.F., Snijder, E.J., Posthuma, C.C., 2011. Discovery of a small arterivirus gene that overlaps the GP5 coding sequence and is important for virus production. J. Gen. Virol. 92, 1097–1106.
Han, M., Du, Y., Song, C., Yoo, D., 2013. Degradation of CREB-binding protein and modulation of type I interferon induction by the zinc finger motif of the porcine reproductive and respiratory syndrome virus nsp1alpha subunit. Virus Res. 172, 54–65.
Han, M., Kim, C.Y., Rowland, R.R., Fang, Y., Kim, D., Yoo, D., 2014. Biogenesis of non-structural protein 1 (nsp1) and nsp1-mediated type I interferon modulation in arteriviruses. Virology 458–459, 136–150.
Han, M., Yoo, D., 2014. Modulation of innate immune signaling by nonstructural protein 1 (nsp1) in the family Arteriviridae. Virus Res. 194, 100–109.
Huang, C., Lokugamage, K.G., Rozovics, J.M., Narayanan, K., Semler, B.L., Makino, S., 2011a. Alphacoronavirus transmissible gastroenteritis virus nsp1 protein suppresses protein translation in mammalian cells and in cell-free HeLa cell extracts but not in rabbit reticulocyte lysate. J. Virol. 85, 638–643.
Huang, C., Lokugamage, K.G., Rozovics, J.M., Narayanan, K., Semler, B.L., Makino, S., 2011b. SARS coronavirus nsp1 protein induces template-dependent endonucleolytic cleavage of mRNAs: viral mRNAs are resistant to nsp1-induced RNA cleavage. PLoS Pathog. 7, e1002433.
Johnson, C.R., Griggs, T.F., Gnanandarajah, J., Murtaugh, M.P., 2011. Novel structural protein in porcine reproductive and respiratory syndrome virus encoded by an alternative ORF5 present in all arteriviruses. J. Gen. Virol. 92, 1107–1116.
Kamitani, W., Huang, C., Narayanan, K., Lokugamage, K.G., Makino, S., 2009. A two-pronged strategy to suppress host protein synthesis by SARS coronavirus nsp1 protein. Nat. Struct. Mol. Biol. 16, 1134–1140.
Kamitani, W., Narayanan, K., Huang, C., Lokugamage, K., Ikegami, T., Ito, N., Kubo, H., Makino, S., 2006. Severe acute respiratory syndrome coronavirus nsp1 protein suppresses host gene expression by promoting host mRNA degradation. Proc. Natl. Acad. Sci. USA 103, 12885–12890.
Kim, O., Sun, Y., Lai, F.W., Song, C., Yoo, D., 2010. Modulation of type I interferon induction by porcine reproductive and respiratory syndrome virus and degradation of CREB-binding protein by non-structural protein 1 in MARC-145 and HeLa cells. Virology 402, 315–326.
Kubota, T., Matsuoka, M., Xu, S., Otsuki, N., Takeda, M., Kato, A., Ozato, K., 2011. PIASy inhibits virus-induced and interferon-stimulated transcription through distinct mechanisms. J. Biol. Chem. 286, 8165–8175.
Kuss, S.K., Mata, M.A., Zhang, L., Fontoura, B.M., 2013. Nuclear imprisonment: viral strategies to arrest host mRNA nuclear export. Viruses 5, 1824–1849.
Lee, S.M., Schommer, S.K., Kleiboeker, S.B., 2004. Porcine reproductive and respiratory syndrome virus field isolates differ in in vitro interferon phenotypes. Vet. Immunol. Immunopathol. 102, 217–231.
Li, Y., Treffers, E.E., Napthine, S., Tas, A., Zhu, L., Sun, Z., Bell, S., Mark, B.L., van Veelen, P.A., van Hemert, M.J., Firth, A.E., Brierley, I., Snijder, E.J., Fang, Y., 2014. Transactivation of programmed ribosomal frameshifting by a viral protein. Proc. Natl. Acad. Sci. USA 111, E2172–E2181.
Li, Y., Zhu, L., Lawson, S.R., Fang, Y., 2013. Targeted mutations in a highly conserved motif of the nsp1beta protein impair the interferon antagonizing activity of porcine reproductive and respiratory syndrome virus. J. Gen. Virol. 94, 1972–1983.
Liu, B., Gross, M., ten Hoeve, J., Shuai, K., 2001. A transcriptional corepressor of Stat1 with an essential LXXLL signature motif. Proc. Natl. Acad. Sci. USA 98, 3203–3207.
Meulenberg, J.J., Hulst, M.M., de Meijer, E.J., Moonen, P.L., den Besten, A., de Kluyver, E.P., Wensvoort, G., Moormann, R.J., 1993. Lelystad virus, the causative agent of porcine epidemic abortion and respiratory syndrome (PEARS), is related to LDV and EAV. Virology 192, 62–72.
Miller, L.C., Laegreid, W.W., Bono, J.L., Chitko-McKown, C.G., Fox, J.M., 2004. Interferon type I response in porcine reproductive and respiratory syndrome virus-infected MARC-145 cells. Arch. Virol. 149, 2453–2463.
Miller, L.C., Lager, K.M., Kehrli, M.E., Jr., 2009. Role of toll-like receptors in activation of porcine alveolar macrophages by porcine reproductive and respiratory syndrome virus. Clin. Vaccin. Immunol. 16, 360–365.
Nedialkova, D.D., Ulferts, R., van den Born, E., Lauber, C., Gorbalenya, A.E., Ziebuhr, J., Snijder, E.J., 2009. Biochemical characterization of arterivirus nonstructural protein 11 reveals the nidovirus-wide conservation of a replicative endoribonuclease. J. Virol. 83, 5671–5682.
Nelsen, C.J., Murtaugh, M.P., Faaberg, K.S., 1999. Porcine reproductive and respiratory syndrome virus comparison: divergent evolution on two continents. J. Virol. 73, 270–280.
Okubo, S., Hara, F., Tsuchida, Y., Shimotakahara, S., Suzuki, S., Hatanaka, H.,

Yokoyama, S., Tanaka, H., Yasuda, H., Shindo, H., 2004. NMR structure of the N-terminal domain of SUMO ligase PIAS1 and its interaction with tumor suppressor p53 and A/T-rich DNA oligomers. J. Biol. Chem. 279, 31455–31461.
Patel, D., Nan, Y., Shen, M., Ritthipichai, K., Zhu, X., Zhang, Y.J., 2010. Porcine reproductive and respiratory syndrome virus inhibits type I interferon signaling by blocking STAT1/STAT2 nuclear translocation. J. Virol. 84, 11045–11055.
Pei, Y., Hodgins, D.C., Lee, C., Calvert, J.G., Welch, S.K., Jolie, R., Keith, M., Yoo, D., 2008. Functional mapping of the porcine reproductive and respiratory syndrome virus capsid protein nuclear localization signal and its pathogenic association. Virus Res. 135, 107–114.
Segundo, F.D., Weiss, M., Perez-Martin, E., Dias, C.C., Grubman, M.J., Santos Tde, L., 2012. Inoculation of swine with foot-and-mouth disease sap-mutant virus induces early protection against disease. J. Virol. 86, 1316–1327.
Snijder, E.J., Kikkert, M., Fang, Y., 2013. Arterivirus molecular biology and pathogenesis. J. Gen. Virol. 94, 2141–2163.
Snijder, E.J., Meulenberg, J.J., 1998. The molecular biology of arteriviruses. J. Gen. Virol. 79, 961–979.
Sokoloski, K.J., Chaskey, E.L., Wilusz, J., 2009. Virus-mediated mRNA decay by hyperadenylation. Genome Biol. 10, 234.
Song, C., Krell, P., Yoo, D., 2010. Nonstructural protein 1alpha subunit-based inhibition of NF-kappab activation and suppression of interferon-beta production by porcine reproductive and respiratory syndrome virus. Virology 407, 268–280.
Subramaniam, S., Kwon, B., Beura, L.K., Kuszynski, C.A., Pattnaik, A.K., Osorio, F.A., 2010. Porcine reproductive and respiratory syndrome virus non-structural protein 1 suppresses tumor necrosis factor-alpha promoter activation by inhibiting NF-kappab and Sp1. Virology 406, 270–279.
Sun, Y., Han, M.Y., Kim, C., Calvert, J.G., Yoo, D., 2012. Interplay between interferon-mediated innate immunity and porcine reproductive and respiratory syndrome virus. Virus-Basel 4, 424–446.
Sun, Y., Li, D., Giri, S., Prasanth, S.G., Yoo, D., 2014. Differential host cell gene expression and regulation of cell cycle progression by nonstructural protein 11 of porcine reproductive and respiratory syndrome virus. Biomed. Res Int. 2014, 430508.
Tohya, Y., Narayanan, K., Kamitani, W., Huang, C., Lokugamage, K., Makino, S., 2009. Suppression of host gene expression by nsp1 proteins of group 2 bat coronaviruses. J. Virol. 83, 5282–5288.
Walsh, D., Mohr, I., 2011. Viral subversion of the host protein synthesis machinery. Nat. Rev. Microbiol. 9, 860–875.
Wensvoort, G., Terpstra, C., Pol, J.M., ter Laak, E.A., Bloemraad, M., de Kluyver, E.P., Kragten, C., van Buiten, L., den Besten, A., Wagenaar, F., et al., 1991. Mystery swine disease in The Netherlands: the isolation of Lelystad virus. Vet. Q. 13, 121–130.
Wootton, S., Yoo, D., Rogan, D., 2000. Full-length sequence of a Canadian porcine reproductive and respiratory syndrome virus (PRRSV) isolate. Arch. Virol. 145, 2297–2323.
Xue, F., Sun, Y., Yan, L., Zhao, C., Chen, J., Bartlam, M., Li, X., Lou, Z., Rao, Z., 2010. The crystal structure of porcine reproductive and respiratory syndrome virus nonstructural protein Nsp1beta reveals a novel metal-dependent nuclease. J. Virol. 84, 6461–6471.
Yoo, D., Song, C., Sun, Y., Du, Y., Kim, O., Liu, H.C., 2010. Modulation of host cell responses and evasion strategies for porcine reproductive and respiratory syndrome virus. Virus Res. 154, 48–60.
Zust, R., Cervantes-Barragan, L., Kuri, T., Blakqori, G., Weber, F., Ludewig, B., Thiel, V., 2007. Coronavirus non-structural protein 1 is a major pathogenicity factor: implications for the rational design of coronavirus vaccines. PLoS Pathog. 3, 1062–1072.